ADVANCED FUNCTIONAL MATERIALS

DOI: 10.1002/adfm.200800073

Limits to Nanopatterning of Fluids on Surfaces in Soft Lithography**

By *Jens A. Wigenius, Mahiar Hamedi,* and *Olle Inganäs**

Soft lithographic microcontact printing using the residual polydimethylsiloxane (PDMS) found in elastomeric PDMS stamps is demonstrated to lead to unstable prints with sub-micrometer dimensions. The statics and dynamics of the process have been followed with time-resolved atomic force microscopy, imaging ellipsometry, water contact angle measurement, and optical diffraction. It is proposed that this instability places a fundamental limitation on patterning by macromolecular fluids, which is of general relevance to soft lithography and nanoimprint lithography with low viscosity polymers.

1. Introduction

The developments of lithography, from photolithography via nanoimprinting lithography (NIL) to soft lithography, rely on the fidelity of patterns generated in thin polymer films on surfaces. In photolithography, pattern generation occurs by photo-initiated chemistry induced in a thin film, and the development of the pattern after light exposure requires physical removal of part of the layer through dissolution. To remove these parts, the photochemistry in a negative photoresist induces increasing solubility by chain scission, or for positive type resists, by decreasing solubility. The stability of the resulting structures is essential, and the materials design avoids the mechanical instabilities found in microstructures. In NIL, and in some soft lithography methods, the pattern transfer exploits a soft or fusible phase of the polymer layer, and the mechanical instabilities of such fluid phases causes limitations to nanopatterning. Here we demonstrate the relevance of the geometrical instability of fluid films on surfaces in nanopatterning using low-molecular-weight oligomers in soft lithographic patterning on surfaces. The instability sets a limit for the fidelity in nanopatterning, and is relevant to pattern transfer in the 100–1000 nm range. This limitation is also relevant to methods of micro and nanopatterning based on mass flow induced by capillary pressure, electric field, or temperature gradients, as analyzed in a rich literature.[1–3] While many of the studies of thin film (in)stability are performed on flat surfaces, following dewetting induced by external forces which lead to structure formation, less attention has been given to the instabilities as they would impact on the formation of standard geometries in nanopatterning. In particular, the uses of patterning for nano- and microelectronics, for photonics, and for biochips are typically directed towards rectangular geometries. In (opto) electronics, including memory functions and processors, thin slender wires are ubiquitous. The aspect ratio (length/width) may be 100 to 1000, for special functions, and therefore the generation of such slender wires is critical. An early instability study of free liquid cylinders, analyzed by Plateau and Rayleigh in the 1890s and properly named the Rayleigh–Plateau instability, showed that these would spontaneously form a line of droplets for sufficiently thin cylinders.[4,5]

Extensive modeling of the morphological instabilities of cylinders is found in the literature[5,6] but the implications for nanopatterning have not been generally acknowledged in the soft lithography literature, to our knowledge. The difficulties of improving soft lithography below 50 nm resolution are well known, but the possibility of nanoimprinting down to 2–5 nm has been demonstrated. These structures are typically rectangular, with an aspect ratio ~1. The elegant demonstration by the group of Rogers of the fidelity in reproducing the geometry of micrometer-long carbon nanotube templates of width and height ~2 nm,[7] or Whitesides replication of vertical features of ~2 nm,[8] seems somehow to avoid this limitation, and indicates that engineering of materials may also lead to paths for nanopatterning at very small dimensions.

The dominant material for stamp fabrication in soft lithography is poly(dimethylsiloxane) (PDMS). It has a low surface free energy, allows gas diffusion, it is chemically inert, transparent and flexible, and can conform to a substrate over a large area.[9] Use of PDMS could lead to contamination by low-molecular-weight residuals on the printed pattern when the stamp is removed.[10–12] The low-molecular-weight residuals contribute to improved results in printing and adsorption

[*] Prof. O. Inganäs, J. A. Wigenius, M. Hamedi
IFM, Linköping University
s.e.-581 83 Linköping (Sweden)
E-mail: ois@ifm.liu.se

[**] The partial support of the EC-funded project NaPa (Contract no. NMP4-CT–2003–500120) is gratefully acknowledged. Funding from the Swedish Strategic Research Foundation SSF through the Center of Organic Electronics (COE) is likewise acknowledged. Instrument grants from the Knut and Alice Wallenberg Foundation made experiments possible. The content of this work is the sole responsibility of the authors.

of biomolecules, and is, therefore, a common element in soft lithographic patterning.[13,14] The degree of contamination of the printed pattern has been shown to be higher when polar inks are used, compared with apolar inks, where the ink could be preventing contamination by shielding the surface.[15] We have obtained results that indicate that the transferred PDMS residuals behave as a fluid during the printing process. Thin lines collapse into droplets, and printed disks collapse into circles. These processes are driven by a process similar to the Rayleigh–Plateau instability to achieve the most favorable free surface energy situation of a fluid nanostructure supported on a solid. We propose that these are fundamental limitations to patterning using macromolecular fluids, and are of general relevance to soft lithography and nanoimprint lithography with low viscosity polymers. While some forms of nanopatterning use higher viscosity polymer layers, a processing step where lower viscosity is obtained at higher temperature is often used, and we, therefore, suggest that the liquid instability could also be of relevance here.

2. Results

2.1. Surface Energy Patterning by Microcontact Printing (μCP) with Bare PDMS

By placing a relief patterned PDMS stamp in conformal contact with a substrate, low-molecular-weight residuals are transferred to the substrate to form a pattern with altered surface energy (Fig. 1), which in turn forms a distinct and stable pattern that is a positive copy of the stamp. The thickness of the transferred material is easily mapped and measured with imaging null ellipsometry (Fig. 2). The PDMS stamp was molded on a photolithographic patterned master. The pattern consisted of 300 μm wide lines standing out 20 μm from the surface, separated 100 μm from each other. The stamp was put into conformal contact with a clean hydrophilic SiO_2 surface, and the substrate examined after stamp removal. A very thin layer of material (0.9 ± 0.2 nm) is transferred within a contact time as short as seconds, on lines where contact between the stamp and the substrate has been achieved. The thickness of the transferred layer was increased with increasing contact

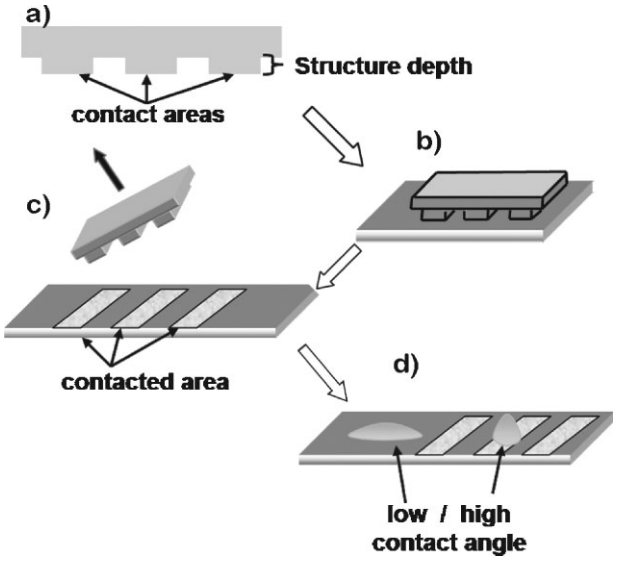

Figure 1. Schematic drawing of μCP with a bare PDMS stamp that leaves residuals in the contacted areas. The structured PDMS stamp (a) is put in contact with a clean hydrophilic substrate (b) and removed to leave low-molecular-weight residuals mainly where contact has been achieved (c) to form a pattern with alternating surface energy (d).

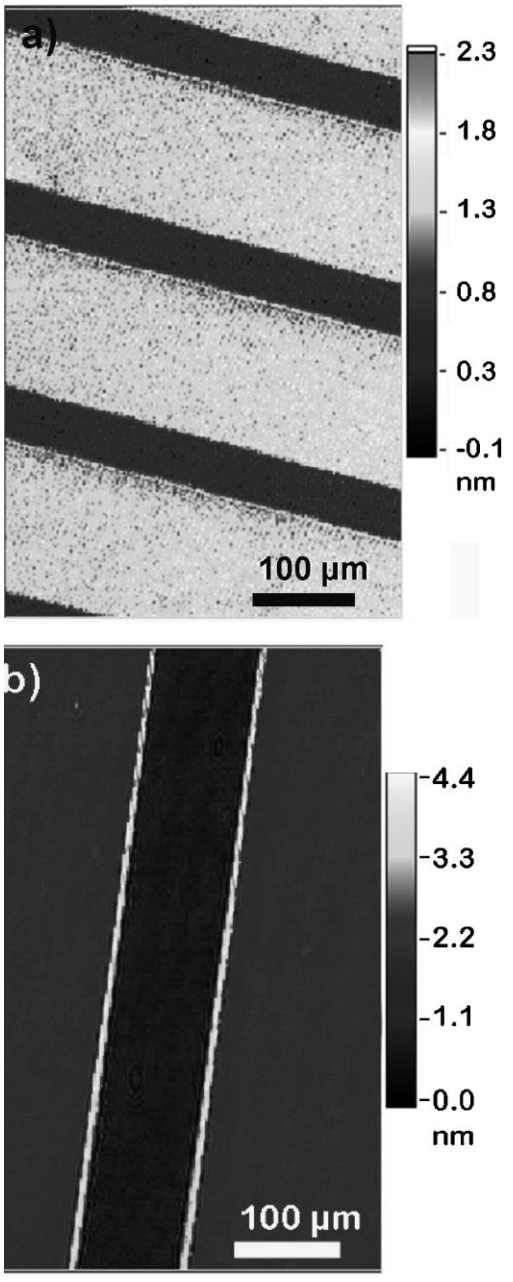

Figure 2. Imaging null ellipsometry picture of SiO_2 substrates after 15 min (a) or 24 h (b) contact time with a relief PDMS stamp.

ADVANCED FUNCTIONAL MATERIALS

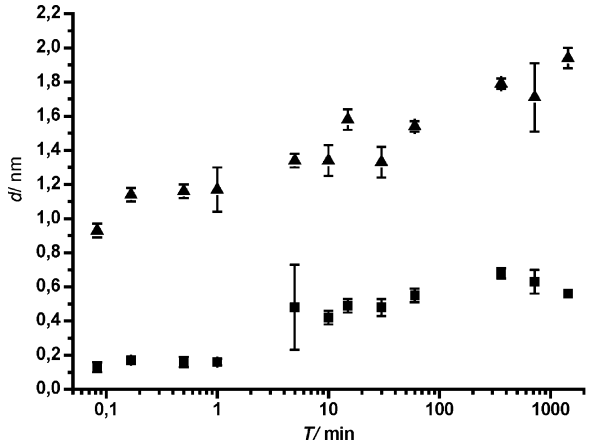

Figure 3. Thickness of the transferred material depending on the contact time between the stamp and the substrate in the contacted areas (▲) and in the non-contacted areas (■) between the ridges measured with imaging ellipsometry.

time. After 15 min it was measured to 1.6 ± 0.2 nm. At longer contact times the growth rate decreased, as can be seen in Figure 3. After 24 h contact time, the thickness of the transferred material is only slightly increased to 1.9 ± 0.2 nm. But as seen in Figure 2b, there are comparably high and sharp ridges formed at the edges of the transferred lines, up to 4.5 nm high. This edge effect has been reported earlier by Wang et al. who measured them with AFM.[12] The valleys found in the transferred pattern correspond to the areas where the stamp has not been in contact with the substrate. The width of the valleys was measured to 100 ± 5 μm, which is also the spacing between the lines on the master. This shows that the transferred pattern corresponds well to the PDMS stamp. The valleys are expected to be hydrophilic and free from PDMS residuals, as reported in earlier studies.[11,12] Nevertheless, with imaging null ellipsometry we could detect a very thin layer of 0.5 ± 0.2 nm after a short contact time of <15 min, of what is believed to be transferred material from the stamp in the valleys. After a longer contact time, 24 h or more, the layer thickness in the valleys has increased to 0.6 ± 0.2 nm. PDMS patterns in this feature size regime appear to be very stable; after one month of storage in room temperature and humidity no significant changes in topography could be observed. Imaging null ellipsometry is a fast method, compared with AFM, to determine the thickness of patterned films. It is also very reliable and has a high resolution in thickness, but less so in lateral dimensions. Nevertheless, the values are extracted from the ellipsometry model and agree very well with AFM thickness measurements (data not shown).

By analyzing a similar PDMS grating pattern, printed on a native SiO_2 substrate, by scanning electron microscopy (SEM) a distinct pattern correlating well with the stamp geometry was measured (Fig. 4). The SEM analysis also showed traces of PDMS between the contacted areas, in this case as a thin and somewhat diffuse line.

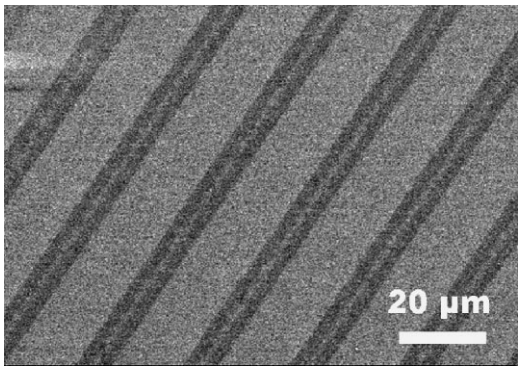

Figure 4. SEM micrograph of a μCP PDMS grating on SiO_2. The dark gray stripes correspond to the separation between the lines on the stamp, and the pale grey where transfer of material has occurred.

2.2. Decreasing Stamp Feature Size, Sub-micrometer

By casting and curing PDMS on commercial optical diffraction gratings, stamps structured with lines at a period of 1200 lines mm^{-1} were manufactured. The cross-section of the line has a sinusoidal shape with a depth of 300 nm and 0.83 μm between the maxima. After placing the stamp in contact with the substrate for 15 min and removing it, AFM measurements were performed. The pattern is well transferred from the stamp to the substrate as can be seen in Figure 5. The ridges have an average thickness of 10 nm and a width of ~400 nm. It is clear that the period is preserved since six ridges are situated in a square of 5 μm. Small dots are observed in the area between the ridges, which are thinner compared with the ridges, <6 nm. These dots are usually, but not always, present, as can be seen in Figure 7a, where an optical grating with 600 lines mm^{-1} (1.67 μm between maxima) was used to print the

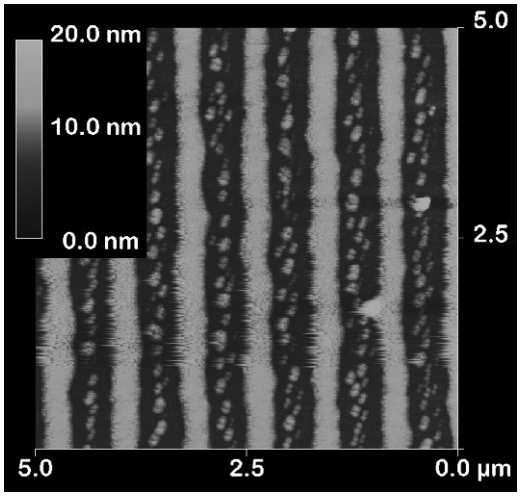

Figure 5. AFM micrograph of μCP with bare PDMS stamps measured directly after μCP, the stamp was molded on an optical grating with a period of 1200 lines mm^{-1} (contact time 15 min and native SiO_2 wafers as substrate).

grating pattern. The thickness of the printed pattern also depends on the feature size of the stamp. With increasing feature size, the height of the printed ridges/bands decreased, from ~15 nm when using 0.83 μm to 2 nm for the 10 μm lines and 1.6 nm with lines of 300 μm, all printed with the same contact time of 15 min. Stamps molded on gratings with a 2400 lines mm^{-1} pattern resulted in irregular and blurred AFM micrographs (data not shown).

Nevertheless, an increase in the period of the printed grating does not significantly affect the contact angle of water (Fig. 6). The water contact angle was $96^\circ \pm 3^\circ$, on a PDMS grating pattern with 300 lines mm^{-1}, as compared with $94^\circ \pm 5^\circ$ on 1200 lines mm^{-1}. A flat stamp print gives a mean contact angle of $66^\circ \pm 4^\circ$. The contact angle of the already hydrophobic glass substrate increased further upon printing of a 300 or 1200 lines mm^{-1} PDMS grating, from $77^\circ \pm 3^\circ$ to $107^\circ \pm 4^\circ$.

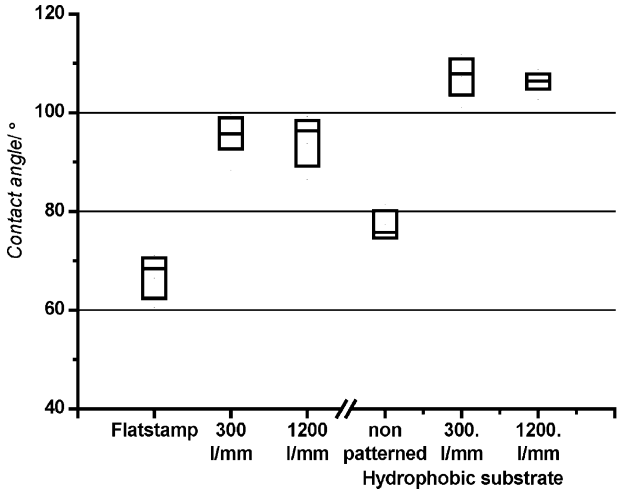

Figure 6. The static water contact angle measurements on PDMS-patterned clean hydrophilic SiO_2 substrates compared with a hydrophobic SiO_2 substrate. The box borders show the standard deviation in relation to the average, the line inside the box.

2.3. Instability in Printed PDMS Patterns

When printing PDMS gratings with a period of ≥600 lines mm^{-1} onto hydrophilic substrates, the printed lines could be split into two parts, one more narrow and one broader line. Also, as mentioned above, several dots are detected in a curved line between the two lines (Fig. 7b). The width and shape of the lines varied greatly, but always with two sharp edges facing each other with a dotted curved line in between. A similar result appeared when patterns of disks 5 μm in diameter and 5 μm apart were used to mould the PDMS stamp. After putting the stamp in conformal contact with a clean SiO_2 surface for 15 min and removing it, a pattern of circles with a diameter of 5 μm was detected by AFM (Fig. 7c).

To determine if this behavior depends on the surface energy of the SiO_2 substrate, clean native substrates were modified by submersion in a dimethyldichlorosilane/xylene solution (1%). After rinsing and ultrasonication in xylene, a monolayer of adsorbed silanes changes the native hydrophilic state of SiO_2 into a hydrophobic state (water contact angle ~80°). The resulting PDMS patterns after printing with a 600 lines mm^{-1}

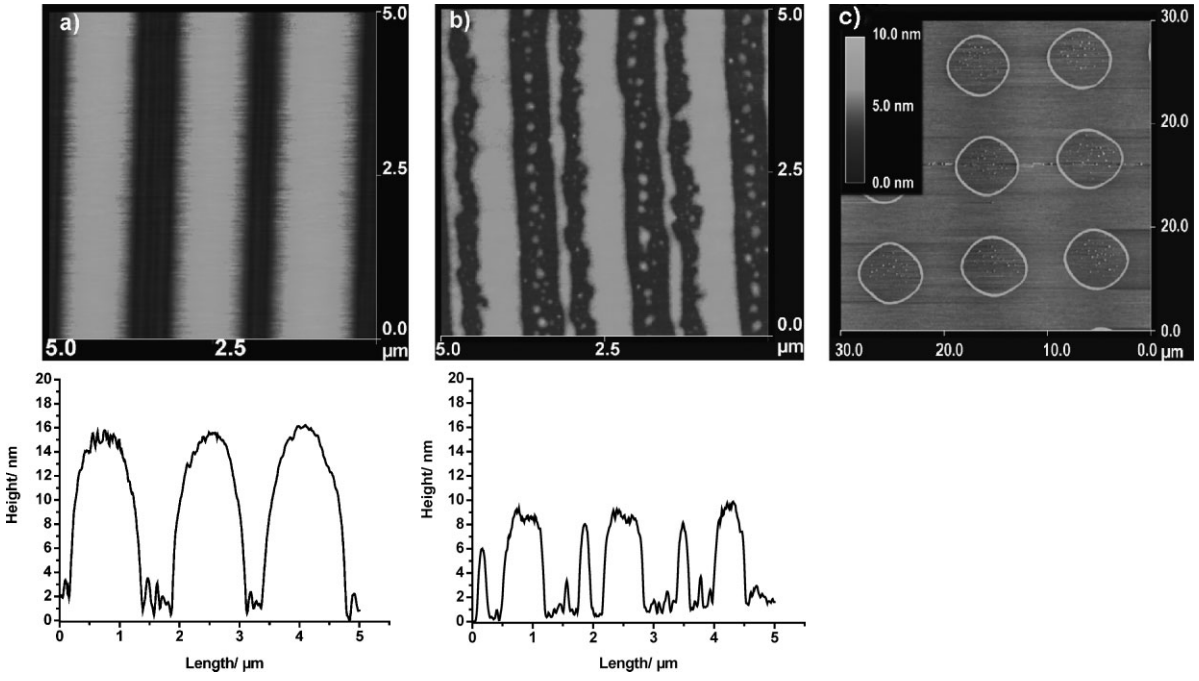

Figure 7. AFM micrograph of μCP with bare PDMS stamps and the profile thickness profile, a) measured directly after μCP, and b) measured two weeks after μCP. The stamp was molded on an optical grating with a period of 600 lines mm^{-1}. c) Disks (5 μm diameter and separated by 5 μm) measured directly after μCP the stamp pattern. In all experiments the contact time was 15 min, and native clean SiO_2 wafers were used.

ADVANCED FUNCTIONAL MATERIALS

PDMS grating stamp was examined with time resolved AFM. The first micrograph was obtained 20 min after the stamp had been removed, the second 20 min later, and the third 50 min later, as shown in Figure 8. Rod-shaped ridges of a few micrometers in length in the 20 min micrograph contracted to oval drops in the 40 min micrograph and finally into spherical drops in the last 90 min micrograph. The final drops are dispersed in diameter but well lined up with the same period as the stamp. In some areas, smaller droplets were detected in two columns, which probably originate from one transferred line that has split in a similar way as in Figure 5b where PDMS was microcontact printed on hydrophilic SiO_2. The heights of the drops are increased compared with the lines on hydrophilic substrates, from ~10 to ~25 nm for the rods, and even more (50 ± 15 nm) for the drops.

This destabilization from a line into drops could not be time resolved with AFM when printing PDMS gratings onto a native hydrophilic SiO_2 surface. However, it could be followed using diffraction of a laser beam in a printed PDMS grating. A PDMS grating stamp (600 lines mm^{-1}) was put in conformal contact with a clean hydrophilic glass slide for 10 min. The printed grating was illuminated with a green laser (λ 543.5 nm) and the intensity of the resulting diffraction pattern was monitored with photodiodes fixed in the diffraction maxima. The intensity at the maxima descends abruptly when the stamp is removed, and it was possible to follow only the first and second diffraction maxima. The decline in intensity flattens out 10 min after the stamp is removed and only slightly decreases during the next 30 min (Fig. 9). When performing the same experiment on a hydrophobic glass slide with a monolayer of silanes, the kinetics was slower. The change was still significant 40 min after the printing step. When using a grating stamp with 1200 lines mm^{-1} no diffraction pattern was visible during the printing step, because sagging occurs between the stamp and the substrate. After removing the stamp a weak intensity maximum appeared where the first diffraction order was expected to be. This shows that although sagging is occurring, the pattern is transferred from the stamp to the substrate. Monitoring the intensity resulted in a slightly dropping linear slope compared with the ones from 600 gratings. During all

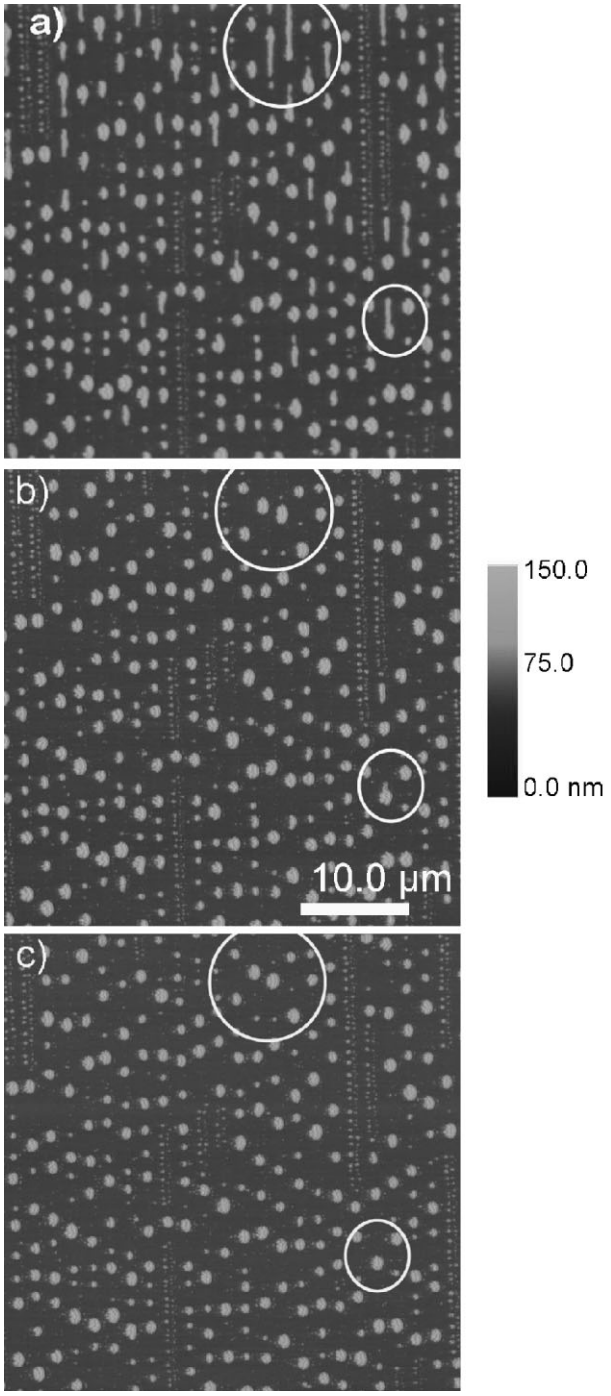

Figure 8. AFM micrograph showing πCP PDMS gratings (600 lines mm^{-1}) on a hydrophobic SiO_2 surface, a) 20, b) 40, and c) 90 min after the stamp has been removed.

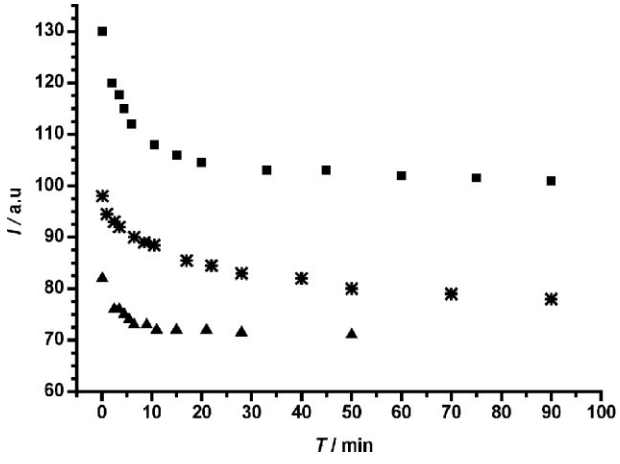

Figure 9. The intensity variation measured with silicon photodiodes of the first (■) and second (▲) orders diffraction maxima from a printed PDMS grating on a hydrophilic glass surface and the first order (⁎) on a hydrophobic glass surface, respectively, depending on the time after stamp the has been removed.

diffraction intensity measurements, the 0^{th} order maxima were monitored to confirm that the laser intensity was constant.

3. Discussion

3.1. Material Transfer

Patterns generated from bare PDMS stamps have been shown earlier by Wang et al. to change the properties of the substrate and to create an alternating pattern of hydrophobic and hydrophilic areas.[12] The modification is a result of low-molecular-weight siloxane residuals that migrate from the bulk of the PDMS stamp to the surface.[11] The amount of transferred material is affected by the type of ink used. Apolar alkanethiol inks have been shown to decrease the contamination level.[15] Low-molecular-weight residuals are also responsible for the hydrophobic recovery of a PDMS stamp surface that is converted into a more hydrophilic state by oxygen plasma treatment.[16,17] However, our SEM micrographs indicate that the transferred material most probably also contains traces of platinum. The high contrast in SEM demands a high electron density component in the residuals; platinum is added to Sylgard 184 as a catalyst to increase the reaction rate during cross linking and is most probably also transferred from the stamp.

To our knowledge, no fast and easy method can completely and permanently remove the low molecular residuals from the stamp, and hence the ability of stamps to transfer PDMS residuals to the substrate. Graham et al. suggested a cleaning procedure approximately one week long,[10] and Thibault et al. use a Soxhlet extractor for several hours,[13] and both show results with no or very little transfer of material from the stamp. However, the hydrophobic recovery after oxygen plasma treatment of a 'clean' PDMS stamp is only slightly affected if stored in air; hence the stamps probably regain their ability to contaminate and transfer PDMS residuals.

Curing over long periods of time does not prevent this behavior; even if the stamp is left at room temperature for at least 48 h, it still results in the same pattern of transferred PDMS residuals. In addition, old stamps stored in ambient atmosphere for one month end up showing the same behavior of PDMS residual transfer during μCP. An elevated curing temperature of the stamp was also tested, and no significant changes in material transfer could be resolved with imaging ellipsometry or AFM. This agrees with the literature where the static water contact angle on a flat μCP PDMS residual surface is slightly decreased, from 110° to ~97° when the curing time is increased from 12 to 28 h while keeping the temperature constant, and from ~104° to ~89° when the curing temperature is increased from 20 to 100 °C. Further extension of the curing time or temperature did not affect the contact angle at all.[13] It should be noted that flat stamps were used and, as could be seen in Figure 6, the μCP pattern has a high impact on the static water contact angle, a change of 30° from non-patterned to a grating pattern.

3.1.1. The Impact of Laplace Pressure

The shape of the stamp could also explain why smaller feature sizes result in a thicker PDMS residual layer. The flow of the low viscosity PDMS residue is dominated by hydrodynamic forces, as described in the appropriate continuum mechanics treatment. A driving force for mass flow is attributed to the Laplace pressure P, which is inversely proportional to a radius of curvature R of the liquid under mass flow, $P \approx \Delta(R^{-1})$. When contact printing, we consider that a residual film of PDMS is confined between the stamp and substrate. The local radius of curvature will be highest at the point of air/stamp/substrate contact, where mass flow will also be largest. This can explain the bulging deposits observed at the edges of lines, for all pattern dimensions. It will also explain the higher mass transfer observed with smaller stamp features, as domains of small radius of curvature cover a larger fraction of the surface.

3.1.2. Pattern Sharpness, Ridges, and Dots

In some cases, imaging ellipsometry detected thin layers of PDMS residuals between the areas that had been in contact with the PDMS stamps. Nevertheless, these thin layers do not seem to be affecting the patterning of proteins for building of biochips, as shown by Asberg et al.[14] But as transfer of PDMS residuals from the stamp occurs directly upon contact and a significant thickness is reached after only a few minutes in the contacted areas, and at the same time this thin layer in the non-contacted areas is also growing with increasing contact time, we suggest that short contact times of less than 2 min is preferable when patterning PDMS as an adhesion layer to obtain a distinct and sharp contrast.

The appearance of PDMS residuals between the contacted areas could be a result of partial sagging of the stamp between the contact areas. Another contributing factor could also be lateral diffusion of low-molecular-weight residuals from the vertical walls where the stamp abruptly loses contact with the substrate, and where the Laplace pressure is highest. Lateral diffusion of PDMS residuals have been proposed to explain the high ridges that appear in Figure 2b; when the contact time is increased, the PDMS residuals migrate from the vertical walls and accumulate at the interface between the stamp and the surface, to form the high ridges. Lateral diffusion of other 'ink' molecules have been observed several times in other studies and is a problem during μCP of alkanethiols, causing blurred and diffuse patterns.[18] However none of these mechanisms, partial sagging or lateral diffusion, is a plausible explanation for the dots that start to appear between the lines when the feature size is decreased as in Figure 4 and 5. The patterns on the grating stamps are sinusoidal. If they were made from a rigid material instead of soft, we would expect very thin contact lines and broad lines of non-contacted areas. In the case of a soft stamp put in contact with the rigid substrate, adsorption forces will deform the stamp and broaden the line of contact. However, if the stamp is sagging or totally deformed, we expect the pattern to disappear and a PDMS layer will cover the whole stamped areas.

ADVANCED FUNCTIONAL MATERIALS

3.2. Instability of Printed PDMS Residual Patterns

The instability of printed patterns caused by partial sagging of the stamp or by lateral diffusion can not explain the doubling of the printed period in Figure 7b compared with Figure 7a, or how we end up with circles in the case of the μCP of a disk in Figure 7c. It could be argued that this is simply a defect in the stamp; but examination of the PDMS stamp used with AFM shows no such defects. Instead we suggest that the soft grating stamp is deformed when the stamp is placed in contact with the substrate, to form a quite broad ~1.3 μm contact area (Figure 7a) and that the final two separated lines originate from this broad line. The rearrangement from one broader ridge into two separate thinner ridges and the formation of droplets between can be explained as follows:

A thin film of a fluid polymer on a smooth surface will under certain conditions be unstable; dewetting of the surface by growing cellular holes will occur. These holes can grow into polygonal patterns and even be broken down into droplet polygonal structures. This phenomenon has been described by Sharma and Reiter for a polystyrene film on silicon wafers, which suggests that the droplets are formed due to Rayleigh instability.[1] If, instead, the polymer film is formed as thin cylindrical ridges, longer than its circumference on a horizontal solid substrate, they could then be pinched off into droplets since this will be the most favored surface free energy situation for the system.[1,4] The reason for this instability is further explained by Sekimoto et al.[6] and a special case that leads to what Powers and Goldstein describe as propagating Rayleigh instability suggest that the drop formation of fluid lines are dependent on competition between the surface tension and viscosity of the system.[5] Similar behavior has been described for inkjet printed lines that become unstable when the contact angle of the liquid is larger than the advancing contact angle,[19] or the fragmentation of copper nanowires into shorter sections.[20] If we assume that the stamp is partly sagging between the contacted areas, a small amount of residuals are transferred to the substrate, and when the stamp is removed this very thin ridge is abruptly rearranged into spherical droplets to gain the most favorable surface free energy situation. We also suggest that the migration of PDMS residuals is larger at the interface between the stamp, substrate, and air, compared with the transfer between the stamp and the substrate. This can explain the high ridges that appear at the interface boundaries after longer contact times (see Fig. 2b and Ref. [12]). As a result of the greater amount of migrated PDMS residuals at the interface, the ridges will be thicker compared with the middle part of the stripe. When the stamp is removed the fluid is forced to reorganize to gain the most favorable energy situation and a propagating instability will force the thinner layer of the middle part of the stripe to be dragged to the edges of the stripe, which results in a split line with rolling edges. A similar situation could also explain the formation of the circles that occur in Figure 7c where a stamp with 5 μm diameter disks is used. More material is transferred at the edges of the contact areas than in the centre of the disks. The transferred PDMS residuals are then spontaneously reorganized into a circle when the stamp is removed; similar instabilities have been described for cylindrical patterns of fluids by Sekimoto et al.[6] The evidence for this type of rearrangement is shown in Figure 8, by AFM measurements on hydrophobic SiO_2. The reorganization from the initially printed grating of PDMS residuals have already begun in the first micrograph measured 20 min after removal of the stamp. In the following micrograph it is clearly visible that the ridges are pinched off into spherical-shaped drops. In some parts of the micrograph the splitting of one original line into two thinner separated lines is also visible, in these cases the resulting droplets are smaller in size. The diffraction measurements give some further information about the rearrangement kinetics. The drop of intensity in the first and second order maxima, during the first minute after the stamp is removed, indicate that a major rearrangement occurs during this time period, especially on the native SiO_2 substrates where the second-order diffraction is decreasing during the first 10 min before it flattens out, while the first-order diffraction maxima continue to decrease significantly for another 20 min. The decrease in intensity of the first-order diffraction maxima is even further extended in time on hydrophobic SiO_2, but the decrease is less dramatic during the first 10 min after the stamp has been removed. This shows that the reorganization is faster on a hydrophilic surface compared with a hydrophobic. Nevertheless, the reorganization is more extended on the hydrophobic surfaces where the lines are completely pinched off into droplets. Together with the long term pattern stability of the patterns with larger feature sizes, it could be stated that the migration of PDMS residuals on a native silicon dioxide surface is restricted to the immediate surroundings on the micrometer and nanometer scale.

4. Conclusions

We have demonstrated that fluid instabilities cause poor fidelity in printing low viscosity fluids with microcontact printing at submicrometer dimensions. We have confirmed that distinct, thin layers of PDMS residuals, which include metal catalyst, are transferred from the PDMS stamp to the substrate during μCP directly when the stamp is put in contact with the substrate. The resulting pattern is stable in the μm regime over time. However, the transferred PDMS residuals behave as a fluid during the printing step and directly after the stamp has been removed. Under certain conditions, such as with very thin lines (sub micrometer) or thin disks, the fluid is unstable and could, according to the Rayleigh–Plateau instability conditions, rearrange into non-regular distorted droplet patterns or circles. PDMS residuals are also transferred from the stamp in areas where no contact has been achieved and these thin residual layers are also unstable and could rearrange into droplets to achieve the most favorable surface energy situation. Such fluid instabilities are more general than just in the case of

PDMS residuals and we suggest that fluid instabilities place fundamental limits on nanopatterning using fluids with low viscosity polymers. This problem may complicate the ambitions to print nano-electronic systems from fluids.

5. Experimental

All chemicals, expect PDMS was bought from Sigma Aldrich and used as received

Master and Stamp Fabrication: The PDMS stamps were molded on two types of masters; the first master type was commercial optical diffraction gratings with an alumina surface. No surface treatment was needed on the gratings since PDMS will not adhere to the alumina surface. The grating used had a sinusoidal wave shaped cross-section. Four different periods was available 300, 600, 1200, or 2400 lines mm^{-1}, which corresponds to a pitch (distance between two maxima) of 3.33, 1.67, 0.89, or 0.44 μm. The distance between the top and the bottom (amplitude) was measured to 350 ± 10 nm with AFM. This was done on a cured PDMS stamp. The second master type was fabricated with standard photolithography methods on a clean native silicon wafer (Topsil, Denmark), using SU-8 (Micro Chem. Corp, USA) as photoresist. To avoid adhesion between this master and the stamp, silanization is necessary. By submerging the master in a solution of xylene (50 mL) and dimethyldichlorosilane (50 μL) for 5 min, followed by extensive rinsing with xylene and ultrasonication for 5 min in Milli-Q water, a thin anti-adhesion layer is formed on the master. Two photolithographically fabricated masters were used, one that contained two rectangular areas of 30 hollow lines in each area with increasing widths from 10 to 400 μm and a constant distance between the hollow lines of 100 μm in the first area, 50 μm in the second area. The depth of the hollow was 20 μm, the stamp is a negative copy of the master. The second had a square that contained a large number of hollow circular disks 5 μm in diameter and separated with 5 μm in orthogonal directions. The stamps were prepared by mixing a two component silicon elastomeric curing agent and base (mass ratio 1: 10), Sylgard 184 (Dow Corning Corp. USA). To avoid trapped air bubbles in the pattern the elastomeric solution was degassed in a vacuum desiccator until no air bubbles were visible before it was cast on to the master. The elastomer was cured in a convection oven for 45 min at 85 °C. After cooling the stamps were gently peeled off from the master and used immediately.

PDMS Surface Energy Modification: The substrates used in this study were standard silicon wafers with a native oxide layer (~1.5 nm thick) and ordinary object glass slides. New substrates were cleaned every day by immersion in a 5:1:1 mixture of double distilled water (18.2 Ω) (Milli-Q), H_2O_2 (30%) and NH_3 (25%), for 10 min at 85 °C, followed by extensive rinsing in Milli-Q water (TL-1 washing procedure). The substrates were stored submerged in Milli-Q water during the day. They were dried in a stream of nitrogen followed by treatment in an oxygen radio frequency (RF) plasma chamber (Pico-RF, Diener electronic, Germany) (30 s, 175 W, 0.05 torr) immediately before the patterning step. RF plasma treatment made the substrates more hydrophilic by introducing hydroxy groups at the surface. A PDMS stamp was then gently brought into conformal contact with the substrate by hand. The contact time varied depending on the specific experiment from a few seconds up to 48 h. If not stated in the text the 10 min contact time was used as a standard. The stamp was then peeled off gently, and only used once (Fig. 1).

Characterization of the Transferred PDMS Pattern:

a) Thickness Measurements. To analyze and measure the thickness of the PDMS patterned substrates we used an imaging null ellipsometer, EP^3 (Nanofilm surface analyse, Germany) and an atomic force microscope (Dimension 3000, Vecco, Digital instruments). The EP^3 is an ordinary null ellipsometer fitted with an *X*,*Y*,*Z* sample holder and CCD camera as detector. This makes it possible to calculate the nulling conditions in every pixel individually with the software (EP^3 View V2.05) and display a map of the ellipsometric parameter, Δ and Ψ, in each pixel. By building a model system of the sample and addressing known refractive indexes (SiO_2 $n = 1.4605$, $k = 0$, PDMS $n = 1.44$, $k = 0$ [21]) and thicknesses for the different layers in the sample is it also possible to calculate and display a map of the layer thickness. The objective used had 2 or 10 times enlargement (2×, 10×), which determined the lateral resolution of the system. Under optimal conditions with a 10× objective this was 1 μm, and the thickness resolution was 0.1 nm. The imaging null ellipsometer measured the film thickness as an average over a defined region of interest (ROI). All thickness measurements have been calculated as an average of at least five ROI measured on five PDMS patterns. The samples were placed on the sample holder and characterized directly after patterning. The samples were illuminated using a laser (λ 532 nm). The angle of incident light was set to 60° and the laser intensity to 2% or 16% for 2× and 10×, respectively. A beam expander was used to increase the illuminated area. A non-patterned and clean area of the substrate was used to determine the SiO_2 thickness of each substrate. To verify the ellipsometry data and to examine lateral submicrometer structures, AFM characterization was performed. NSG 10 cantilevers (NT-MDT, Netherlands) were used in tapping mode and the measurements were evaluated with the software V5.30 (Digital instruments).

b) Scanning electron microscopy (SEM). PDMS residuals were patterned on pure Si substrates by placing the stamp in contact with the Si substrate for some minutes and removing the stamp. The PDMS stamps were prepared by molding from a master that contained a micro-patterned SU-8 resist on Si. No metal was evaporated on top of the patterned Si substrate. SEM pictures were taken from PDMS-patterned Si using a LEO 1550 Gemini (Leo Elektronenmikroskopie GmbH, Germany) with 5.00 KV electron beam power and a secondary electron detector.

c) Contact angle goniometry. Contact angle goniometry with a CAM 200 goniometer (KSV Instruments, Finland) was used to analyze the influence on the surface wettability of the substrates before and after being patterned with PDMS gratings, using fresh Milli-Q water at room temperature and the humidity of the ambient air. The substrates were cleaned and patterned as described above. To achieve hydrophobic substrates, TL-1 washed SiO_2 substrates were submerged in a solution of xylene (50 mL) and dimethyldichlorosilane (50 μL) for 5 min, followed by extensive rinsing with xylene and ultrasonication for 5 min in Milli-Q water. On every surface, water droplets of a similar size were placed and their contact angles with the surfaces were measured.

d) Light diffraction. Light diffraction was performed in a dark room and used to follow the rearrangement in the printed PDMS gratings. A PDMS grating was printed onto a glass substrate as described above. The PDMS grating-patterned glass slide was placed in the laser beam (λ 534.5 nm). The resulting diffraction pattern was observed; silicon photodiodes were placed at the first and second intensity maxima, the photo voltage was measured with a digital multimeter and plotted relative to the time after stamp removal. The transmitted laser intensity was also measured to detect any change in the incident light.

Received: January 15, 2008
Revised: March 3, 2008
Published online: August 20, 2008

[1] A. Sharma, G. Reiter, *J. Colloid Interface Sci.* **1996**, *178*, 383.
[2] G. Reiter, M. Hamieh, P. Damman, S. Sclavons, S. Gabriele, T. Vilmin, E. Raphael, *Nat. Mater.* **2005**, *4*, 754.
[3] N. E. Voicu, S. Harkema, U. Steiner, *Adv. Funct. Mater.* **2006**, *16*, 926.

ADVANCED FUNCTIONAL MATERIALS

[4] L. Rayleigh, *Proc. Lon. Math. Soc.* **1878**, *10*, 4.
[5] T. R. Powers, R. E. Goldstein, *Phys. Rev. Lett.* **1997**, *78*, 2555.
[6] K. Sekimoto, R. Oguma, K. Kawasaki, *Ann. Phys.* **1987**, *176*, 359.
[7] F. Hua, Y. G. Sun, A. Gaur, M. A. Meitl, L. Bilhaut, L. Rotkina, J. F. Wang, P. Geil, M. Shim, J. A. Rogers, A. Shim, *Nano Lett.* **2004**, *4*, 2467.
[8] B. D. Gates, G. M. Whitesides, *J. Am. Chem. Soc.* **2003**, *125*, 14986.
[9] B. D. Gates, Q. B. Xu, M. Stewart, D. Ryan, C. G. Willson, G. M. Whitesides, *Chem. Rev.* **2005**, *105*, 1171.
[10] D. J. Graham, D. D. Price, B. D. Ratner, *Langmuir* **2002**, *18*, 1518.
[11] K. Glasmastar, J. Gold, A. S. Andersson, D. S. Sutherland, B. Kasemo, *Langmuir* **2003**, *19*, 5475.
[12] X. J. Wang, M. Ostblom, T. Johansson, O. Inganas, *Thin Solid Films* **2004**, *449*, 125.
[13] C. Thibault, C. Severac, A. F. Mingotaud, C. Vieu, M. Mauzac, *Langmuir* **2007**, *23*, 10706.
[14] P. Asberg, K. P. R. Nilsson, O. Inganas, *Langmuir* **2006**, *22*, 2205.
[15] R. B. A. Sharpe, D. Burdinski, C. van der Marel, J. A. J. Jansen, J. Huskens, H. J. W. Zandvliet, D. N. Reinhoudt, B. Poelsema, *Langmuir* **2006**, *22*, 5945.
[16] M. J. Owen, P. J. Smith, *J. Adhes. Sci. Technol.* **1994**, *8*, 1063.
[17] H. Hillborg, U. W. Gedde, *Polymer* **1998**, *39*, 1991.
[18] E. Delamarche, H. Schmid, A. Bietsch, N. B. Larsen, H. Rothuizen, B. Michel, H. Biebuyck, *J. Phys. Chem. B* **1998**, *102*, 3324.
[19] P. C. Duineveld, *J. Fluid Mech.* **2003**, *477*, 175.
[20] M. E. Toimil-Molares, A. G. Balogh, T. W. Cornelius, R. Neumann, C. Trautmann, *Appl. Phys. Lett.* **2004**, *85*, 5337.
[21] N. K. Persson, O. Inganas, *Sol. Energy Mater. Sol. Cells* **2006**, *90*, 3491.